



Porous defect-modified graphitic carbon nitride via a facile one-step approach with significantly enhanced photocatalytic hydrogen evolution under visible light irradiation



Di Zhang, Yongle Guo, Zhongkui Zhao*

State Key Laboratory of Fine Chemicals, Department of Catalysis Chemistry and Engineering, School of Chemical Engineering, Dalian University of Technology, 2 Linggong Road, Dalian 116024, China

ARTICLE INFO

Keywords:

Graphitic carbon nitride
Porous and defect
One-step strategy
Hydrogen evolution
Photocatalysis

ABSTRACT

Graphitic carbon nitride ($g\text{-C}_3\text{N}_4$) has been considered as one of the most promising photocatalysts for solar energy conversion. However, the intrinsic drawbacks of insufficient visible-light absorption and poor charge separation efficiency seriously limit its practical applications in visible light photocatalytic hydrogen evolution. In this work, a facile one-step strategy was proposed to construct a novel porous defect-modified graphitic carbon nitride (P-DCN) via thermal polymerization of a freeze-dried crystalline mixture containing dicyandiamide (DCDA) and ammonium chloride (NH_4Cl) under nitrogen atmosphere, in which both porous feature and two types of defects (cyano group and nitrogen vacancy) were simultaneously introduced into $g\text{-C}_3\text{N}_4$ framework. Results show that the as-synthesized P-DCN exhibits 26 times higher hydrogen evolution rate (HER) under visible light irradiation than bulk $g\text{-C}_3\text{N}_4$, reaching $20.9 \mu\text{mol h}^{-1}$. In combination of porous and defective characteristics, P-DCN even demonstrates 2.0 and 1.8 folds higher HER than highly active porous graphitic carbon nitride (P-CN) and defect-modified $g\text{-C}_3\text{N}_4$ (DCN), respectively. The outstanding photocatalytic performance for hydrogen production originates from the remarkably improved visible light harvesting capability, the notably promoted separation and recombination inhibition of photoinduced charge carriers, and the increased amount of active sites and the strengthened mass transfer resulting from the combination effect of the porous feature, as-formed defects, and the enlarged specific surface area. Moreover, this approach could render a new insight for designing highly efficient visible light photocatalysts for the other transformations including CO_2 reduction, environmental remediation, and organic synthesis process.

1. Introduction

Since the pioneering work of Fujishima and Honda on photoelectrochemical water splitting, inorganic semi-conductive materials used to address global energy and environmental issues have received great interdisciplinary attentions [1]. Amongst inorganic semi-conductive materials, the potential visible-light-active photocatalysts suitable for hydrogen and oxygen produced include metal and nonmetal mixed oxides, sulfides, nitrides [2,3]. These achievements have promoted the development of both solar energy conversion and environmental remediation markedly, but are still far from meeting industrial requirement. Future practical applications have been hampered by its low photocatalytic activity resulting from the large band gap energy and rapid recombination of photoinduced electron-hole pairs [4]. Meanwhile, as the environmental and economic concepts attach more emphases on environmental beginning, low cost, and easy availability,

pursuing an efficient, sustainable and earth-abundant metal-free visible-light active photocatalyst has become a new research hotspot in the field of solar energy conversion.

Owing to the outstanding optical and electronic properties, remarkable thermal and chemical stability, low cost and facile preparation, $g\text{-C}_3\text{N}_4$ has attracted considerable and continuously increasing interest in diverse photocatalytic applications [2–4], since it was utilized as a metal-free visible-light-sensitive photocatalyst in 2009 [5]. All of the aforementioned advantages endow it with extended applications in entire kinds of photocatalytic branches, such as hydrogen and oxygen evolution from water splitting [6–8], contaminant elimination [9,10], organic synthesis [11,12], CO_2 reduction [13–15], H_2O_2 generation [16,17], etc. Nevertheless, the photocatalytic performance of pristine $g\text{-C}_3\text{N}_4$ was generally restricted by the relatively narrow visible light responsive region, fast recombination of photoinduced electron-holes pairs, and low specific surface area caused by highly stacked

* Corresponding author.

E-mail address: zkzhao@dlut.edu.cn (Z. Zhao).

layers [2]. Therefore, many strategies including heteroatom-doping [18–21], thermal and liquid exfoliation [22,23], heterojunction formation [24–26], morphology construction [27,28], supramolecular preorganization [20,29] and dye sensitization [30,31], have been proposed to enhance its photocatalytic performance. Although great and fruitful efforts have been made, the further improvement in photocatalytic efficiency is still required.

From references, the introduction of defects into $g\text{-C}_3\text{N}_4$ framework can efficiently promote its photocatalytic performance [32–38]. It was validated that, the defects in the tri-s-triazine repeating units of $g\text{-C}_3\text{N}_4$ not only function to modify the band structure by generating additional energy level in the band gap, but also serve as trapping sites for photoinduced charge carriers to suppress the recombination of electrons and holes. Diverse strategies such as KOH assisted polymerization, and post-treatment with reductive atmosphere or oxidant were developed to yield defects on $g\text{-C}_3\text{N}_4$. However, each of these strategies has intrinsic drawbacks, such as the required additives, difficultly handling owing to the use of reducing or oxygenated agent, and/or multi-step preparation process, besides relatively low surface area of the as-synthesized $g\text{-C}_3\text{N}_4$. Therefore, the search for a facile strategy for developing defect-modified $g\text{-C}_3\text{N}_4$ with high specific surface area is highly desirable.

Moreover, it was proposed that the introduction of porous characteristic into $g\text{-C}_3\text{N}_4$ could enlarged its specific surface area, promoted light absorption by the multiple scattering effects and the strengthened the mass-transfer. As a consequence, the photocatalytic of $g\text{-C}_3\text{N}_4$ was remarkably improved [19,39–47]. Up to now, various methods have been proposed to synthesized porous $g\text{-C}_3\text{N}_4$, which include hard template [39,40], soft template [41], gaseous template [12], acid treatment [13,42,43], and thermal polymerization assisted by sulfur [44], sucrose [45] and PVP [46], and the freeze-drying assisted processes [47–49].

From above analysis, we envisioned that a defect-modified porous $g\text{-C}_3\text{N}_4$ can exhibit outstanding photocatalytic performance under visible light. However, to the best of our knowledge, there is only a few report on the preparation and photocatalytic application of porous defect-modified $g\text{-C}_3\text{N}_4$ to be found [19,50]. In this work, we firstly describe a facile one-step strategy to fabricate porous $g\text{-C}_3\text{N}_4$ with defects through thermally polymerizing the freeze-dried DCDA- NH_4Cl mixed crystals under the nitrogen atmosphere. Unlike previous report that NH_4Cl generally acted as an efficient exfoliating agent to produce $g\text{-C}_3\text{N}_4$ nanosheets [51,52], in this work, we found that it played an important role in occupying space to limit the long-range polymerization and thus defects had been introduced during the thermal polymerization process, as depicted schematically in Fig. 1. Furthermore, it is expected that the introduction of freeze drying technology may further strengthen the effect of occupying space of NH_4Cl . Moreover, the combination of NH_4Cl assist and the freeze drying technology can also produce pores in $g\text{-C}_3\text{N}_4$. As a consequence, the porous defect-modified $g\text{-C}_3\text{N}_4$ photocatalyst was successfully prepared. The as-synthesized P-DCN Exhibits 26 times higher HER under visible light irradiation than bulk $g\text{-C}_3\text{N}_4$, reaching $20.9 \mu\text{mol h}^{-1}$. It even demonstrates 2.0 and 1.8 folds higher HER than highly active porous graphitic carbon nitride (P-CN) and

defect-modified $g\text{-C}_3\text{N}_4$ (DCN), respectively. To correlate the catalytic performance with the characterization results concerning the structural, textural and photoelectrical properties, the much superior photocatalytic performance can be ascribed to the remarkably improved visible light harvesting capability, the notably promoted separation and recombination inhibition of photoinduced charge carriers, and the increased amount of active sites and the strengthened mass transfer resulting from the combination effect of the porous feature, as-formed defects, and the enlarged specific surface area. Moreover, it is expected that our findings will open a new horizon to design novel and highly efficient metal-free $g\text{-C}_3\text{N}_4$ -based catalysts for photocatalytic and the other applications.

2. Experimental

2.1. Materials and reagents

DCDA was purchased from Tianjin Guangfu Fine Chemical Research Institute, China. NH_4Cl was supplied by Tianjin Bodi Chemical Engineering Co., Ltd., China. Triethanolamine (TEOA) was provided by Aladdin Industrial Corporation. Terpineol was supplied by Tianjin Damao Chemical Reagent Factory. Ultrapure N_2 gas (purity 99.999%) was purchased from Dalian Guangming Special Gas Co., Ltd., China. All reagents used in this study were at least in analytical grade without further purification. De-ionized water was used for all experiments.

2.2. Preparation of photocatalysts

P-DCN was synthesized by thermal polymerizing of the freeze-dried DCDA and NH_4Cl mixed crystals. In detail, DCDA and NH_4Cl were added into 40 mL de-ionized water and froze in liquid nitrogen, and then complex crystal was obtained. The resulting complex crystal was dried in the vacuum freezer dryer to obtain dried mixture. Then, the dried mixture was heated in N_2 flow at 550°C for 4 h under the ramp rate of $3^\circ\text{C}/\text{min}$. Defect-modified $g\text{-C}_3\text{N}_4$ (DCN) was prepared as follows: DCDA and NH_4Cl were put into 40 mL de-ionized water and evaporate the water at 100°C . Then the dried mixture was heated in N_2 flow at 550°C for 4 h at a ramp rate of $3^\circ\text{C}/\text{min}$. For comparison, bulk $g\text{-C}_3\text{N}_4$ (Bulk CN) was synthesized by directly heating DCDA without NH_4Cl in flowing N_2 atmosphere. In addition, for comparison, porous $g\text{-C}_3\text{N}_4$ (P-CN) was prepared according to a previously reported procedure with DCDA instead of melamine [53].

2.3. Photocatalyst characterizations

Transmission electron microscopy (TEM) images were obtained by using a JEM-2000EX TEM instrument (JEOL Co. Ltd.). Scanning electron microscopy (SEM) was performed on a JEOL JSM-5600LV SEM instrument. The crystalline structure of the as-prepared photocatalysts was analyzed using powder X-ray diffraction (XRD) technology on Rigaku Automatic X-ray Diffractometer (D/Max 2400) equipped with a $\text{Cu K}\alpha$ source ($\lambda = 1.5406 \text{ \AA}$). Fourier transform infrared (FTIR) spectroscopy characterization of catalysts was performed at a Bruker EQUINOX55 infrared spectrometer. X-ray photoelectron spectroscopy (XPS) measurements were obtained using an ESCALAB 250 XPS system with a monochromatized $\text{Al K}\alpha$ X-ray source (15 kV, 150 W, 500 mm, pass energy = 50 eV). All binding energies were calibrated to the C 1s peak at 284.6 eV of the surface adventitious carbon. Nitrogen adsorption and desorption isotherms were measured on a Beishide apparatus of model 3H-2000PS1 system at 77 K. Before the measurement, all samples were degassed at 130°C for 8 h. The specific surface areas were calculated via the BET method, and the pore size distributions were calculated from an adsorption branch of the isotherm via the BJH model. The UV–vis diffuse reflectance spectra (DRS) were recorded on a UV–vis spectrometer (JASCO V-550) and were converted from reflection to absorbance by the Kubelka–Munk method. The room-

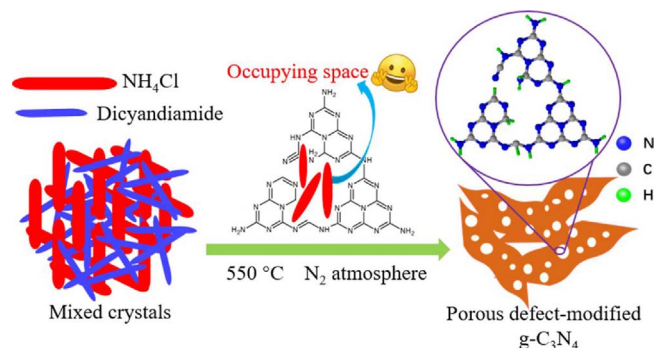


Fig. 1. Schematic illustration for the formation of porous defect-modified $g\text{-C}_3\text{N}_4$.

Download English Version:

<https://daneshyari.com/en/article/6498595>

Download Persian Version:

<https://daneshyari.com/article/6498595>

[Daneshyari.com](https://daneshyari.com)